LOW-FREQUENCY IMPEDANCE CHARACTERISTICS OF A LANGMUIR PROBE IN A PLASMA

by

F. W. Crawford and R. Grard

Rec'd 4/12/65

Internal Memorandum
M. L. Report No. 1294
NSF Grant GP-936
and
NASA Grant NsG 174-61
February 1965

Microwave Laboratory
W. W. Hansen Laboratories of Physics
Stanford University
Stanford, California

LOW-FREQUENCY IMPEDANCE CHARACTERISTICS OF A LANGMUIR PROBE IN A PLASMA*

by

F. W. Crawford
Institute for Plasma Research

and

R. Grard
Radioscience Laboratory

Stanford University
Stanford, California

ABSTRACT

22196

Measurement of the low-frequency impedance of a Langmuir probe in a plasma can give the local electron density and temperature. Such diagnostic methods have been employed in ionospheric probing, but the interpretation of the results based on simplified theory has not been entirely satisfactory. This paper describes laboratory plasma studies designed to investigate the validity of the simplified theory. Good agreement is obtained between results obtained by two different impedance techniques, and conventional Langmuir probe data reduction. It is concluded that the methods could provide additional methods of measurement in laboratory plasmas, with some inherent advantages, but that a more detailed theory and extensive experimental verification are required before they can be applied with confidence to more complicated conditions in the ionosphere.

Author

* This work was supported by the National Science Foundation and NASA.

TABLE OF CONTENTS

LIST OF FIGURES

I. INTRODUCTION

The Langmuir probe has been one of the most important diagnostic tools for measuring electron density and temperature in laboratory plasmas since its development in the 1920's by Langmuir and Mott-Smith. In recent years, its use has been extended to ionospheric and space studies. These have posed new problems concerned with data evaluation and telemetering, and have stimulated research into ways to obtain electron density and temperature measurements rapidly and continuously other than by interpretation of the usual semilogarithmic probe current/potential characteristics. One product of this work is the resonance probe,[1] by which rf impedance effects are studied at frequencies somewhat below the electron plasma frequency. It has also been suggested that data on the low-frequency impedance of a probe in a plasma might be used to obtain electron density and temperature.[2-5] This topic forms the subject of the present paper.

If the low-frequency impedance is measured between a probe and a reference electrode, two extreme conditions can be distinguished: that in which the impedance of the plasma substantially unperturbed by the probe dominates, and that in which local space-charge sheaths around the electrodes constitute the most important impedance components. Which of these is approached in an experimental situation will depend on the electrode sizes and separation, and on the measuring frequency. Similarly, the theoretical treatment required will differ widely for the

two cases. The former can be handled using the effective plasma permittivity concept, while the latter requires knowledge of the sheaths surrounding the electrodes.

In 1962, Mlodnosky and Garriott[2] predicted the existence of parallel resistive and capacitive components of low-frequency sheath impedance, and suggested two ionospheric diagnostic techniques based on measurements of the impedance of a dipole antenna carried by a rocket or satellite. A detailed theory of the impedance was developed subsequently by Crawford and Mlodnosky.[3] Measurements with rocket-borne probes were carried out in 1963 by Stanford Research Institute,[4] and by the University of Pennsylvania.[5] In the latter case, the experimental results were interpreted in terms of the plasma impedance rather than of the sheath. In both cases there were certain discrepancies between theoretical and experimental results which cast doubts on the validity of the relevant theories.

A precise impedance theory for a rocket-borne probe is very difficult to derive: the geometry of the probe is not simple because of aerodynamic effects; the vehicle may have a velocity comparable to the ion thermal velocity so that a shock wave is produced ahead of it and a trail is left behind it, also the magnetic field of the earth may influence the impedance strongly. In the ionosphere, for example, the electron gyroradius can be comparable to the Debye length.

It is desirable that techniques intended for use in the complicated conditions encountered in space probing should be tested in the laboratory under simpler and more controllable conditions to see how closely the theory fits the experimental results. The work described here has been

carried out with these considerations in mind, and has been directed towards verifying the probe impedance theory in the absence of a static magnetic field. Evidence from previous measurements in low-pressure mercury-vapor discharges of the sort used in these experiments shows that when the plasma volume impedance dominates, the results can be explained satisfactorily by equivalent permittivity considerations.[6] Consequently, the concentration here will be on electrode sheath impedance effects. The simplified theory is discussed in Section II, and the experiments are described in Section III. The paper concludes with a brief discussion of the utility of low-frequency probe impedance measuring techniques.

II. PROBE IMPEDANCE THEORY

To indicate the differences in treatment, the probe/plasma impedance theory will be outlined for plasma-dominated conditions, where sheath effects are negligible, as well as for the sheath-dominated case directly related to our experiments. It will be noted that as the cold plasma permittivity is used in the former case, information on electron density and collisions only can be obtained. The sheath-dominated case provides electron density and temperature information, but gives no information on collisions.

A. PLASMA-DOMINATED

The simplest theoretical results are obtained when certain geometrical electrode symmetries can be employed and the capacitance with plasma present can be simply related to that in free space. We have for the probe capacity, C_s ,

$$C_s = \frac{\int_S \sigma dS}{\int_L \underset{\sim}{E} \cdot d\underset{\sim}{L}} = \frac{\int_S \underset{\sim}{D} \cdot d\underset{\sim}{S}}{V} \quad , \tag{1}$$

where L is an arbitrary path between the electrodes, S is the probe surface area, σ is the surface charge density, $\underset{\sim}{E}$ is the electric field, and $\underset{\sim}{D}$ is the electric displacement. The ratio of the capacitance with plasma present, C_p , to that with free space as dielectric, C_0 , is

$$\frac{C_p}{C_0} = \frac{\int_S \underset{\approx}{\epsilon} \underset{\sim}{E} \cdot d\underset{\sim}{S}}{\epsilon_0 \int_S \underset{\sim}{E} \cdot d\underset{\sim}{S}} \quad . \tag{2}$$

The complex plasma permittivity tensor, $\underset{\approx}{\epsilon}$, includes the effects of magnetic field and collisions.

If the geometry is such that the electric field at the electrode surface is everywhere the same in both numerator and denominator, Eq. (2) simplifies to

$$\frac{C_p}{C_0} = \frac{\epsilon_p}{\epsilon_0} \quad . \tag{3}$$

Such conditions would hold, for example, if infinite parallel plane geometry were approached, or if coaxial cylinders oriented along the magnetic field lines were employed. In the first case, ϵ_p can be replaced by the permittivity parallel $(\epsilon_{\parallel})$ or perpendicular $(\epsilon_{\perp})$ to the magnetic field, for plates oriented perpendicular or parallel to the magnetic field; and in the second would be replaced by $\epsilon_{\perp}$. In other geometries, the problem may become extremely complicated. Solution of Laplace's equation in the anisotopic medium and matching to perhaps awkwardly shaped boundaries are then required.

B. SHEATH-DOMINATED

The impedance may be obtained by considering an arbitrary probe characteristic of the form[3]

$$i = f(V) \quad , \tag{4}$$

where i and V contain dc and small-amplitude, time-varying components, denoted by subscripts 0 and 1 , respectively. Expansion by Taylor's theorem gives

$$i_0 + i_1(t) = f(V_0) + V_1(t)\, f'(V_0) + \frac{V_1(t)^2}{2!} f''(V_0) \cdots \quad , \tag{5}$$

which has been studied elsewhere for general noise signals.[7] For a sinusoidal modulating signal we have

$$V_1(t) = V_1 \sin \omega t \quad , \quad i_1(t) \approx V_1 f'(V_0) + \frac{V_1^3}{8} f'''(V_0) \quad . \tag{6}$$

Expressed as a conductance, G_e , this yields

$$G_e(V_0) \approx f'(V_0) \left[1 + \frac{V_1^2}{8} \frac{f'''(V_0)}{f'(V_0)} \right] \quad . \tag{7}$$

For a Maxwellian electron velocity distribution, the probe current in the electron-repelling region will be

$$i = i_e \exp\left(\frac{V}{V_e}\right) + i_i \quad , \tag{8}$$

where i_e and i_i are the electron saturation current and ion current drawn by the probe, respectively, V_e is the electron temperature, and V is the probe potential relative to space potential. If the derivative of the rf component of ion current is neglected as small compared to that of the exponential variation of electron current over the range of experimental interest, and if we assume that the electrons can follow

low-frequency fluctuations instantaneously, then Eq. (7) becomes

$$G_e(V_0) \approx \frac{i_0}{V_e} = \frac{i_e}{V_e} \exp\left(\frac{V_0}{V_e}\right) \quad . \tag{9}$$

Evaluation of the second term in Eq. (7) indicates that Eq. (9) is accurate to one percent for $V_1 < 0.3\ V_e$.

Account must be taken of the displacement current, i_d , which flows while the probe surface charge adjusts to follow the time-varying potential. We have

$$i_d = \frac{d(CV)}{dt} = C\frac{dV}{dt} + V\frac{dC}{dt} \quad , \tag{10}$$

where C is the probe/plasma capacitance. The quantity (dC/dt) is non-zero since the charge distribution which determines C is changing in response to potential variations. If the electrons follow almost instantaneously, then C is a function of V only and Eq. (10) becomes

$$i_d = \left[\frac{d(CV)}{dV}\right]\frac{dV}{dt} = C_e(V)\frac{dV}{dt} \quad . \tag{11}$$

In this, $C_e(V)$ represents a voltage-dependent effective probe/plasma capacity. By Taylor's theorem, we obtain

$$C_{e0} = C_e(V_0) + \frac{V_1^2}{4} C_e''(V_0) + \ldots \quad . \tag{12}$$

In the small-signal limit, $C_e(V)$ in Eq. (11) may be replaced by $C_e(V_0)$. The effective probe admittance, $Y(V_0)$, is obtained by combining this result with Eq. (9). This gives

$$Y(V_0) = G_e(V_0) + j\omega C_e(V_0) \quad . \tag{13}$$

The possible utility of an impedance diagnostic technique depends on the ease and precision with which the quantities $G_e(V_0)$ and $C_e(V_0)$ can be defined and measured. We must now examine them in more detail:

Conductance, $G_e(V_0)$ The expression of Eq. (9) applies to an exponential probe characteristic, and under conditions where the derivative of the ion current component is negligible. For large plane probes this would be so down to very negative probe potentials, because the ion current is substantially independent of probe potential. For cylindrical and spherical geometries the range of operation would be smaller. In any case, practical application of the method is unlikely to be feasible at potentials much below floating potential since the tail of the electron velocity distribution will become progressively more non-Maxwellian and the derivative of the electronic component will become useless as a means of determining electron temperature. We may assume, then, that the range of measurement will be from some point near floating potential, set by the limits within which the tail may be regarded as Maxwellian, to space potential.

It was pointed out by Mlodnosky and Garriott[2] that a useful diagnostic technique can be based on Eq. (9). Below space potential, a plot of conductance against probe current should give a straight line, the

slope of which yields the electron temperature. Above space potential there should be an abrupt change of conductance due to probe saturation effects, although it may be expected that the knee will be smoothed in practice for the same reasons that the saturation knee is smoothed in the conventional semi-logarithmic dc probe characteristic.[8] Location of space potential defines the electron density in the plasma.

Capacitance, $C_e(V_0)$ Under circumstances where it is not feasible to sweep the probe potential, for example in transient plasmas, this operation may be replaced by measurement of the probe capacitance. It is to be expected that the simplest condition will be of most interest in practice, i.e., the capacitance will be measured at floating potential. The approximate theory which follows is rather more general, but the experiments have been restricted to this operating point.

The determination of $C_e(V_0)$ depends on solution of Poisson's equation in the sheath region. Since there is no distinct separation of sheath from plasma, and solution of the full plasma-sheath equation of Tonks and Langmuir[9] is extremely difficult, suitable approximations are required. We shall restrict ourselves to cases in which the sheath thickness is small compared to the probe dimensions. Under this assumption the theory for plane geometry will be approached in non-planar geometries. Next, we shall examine two models which may be expected to bracket the experimental results over the range of interest. The first (I) of these has been applied by Butler and Kino[10] with considerable success to rf sheath behavior in which it can be assumed that the time variation of potential is too rapid for the ions to follow. The second (II) estimates the capacitance at frequencies sufficiently low for both ions and electrons to respond without appreciable delay.

In Model I, it is assumed that the sheath has a thickness, x, given approximately by Child's law for a space-charge-limited ion diode. We have, then,

$$x = \frac{2}{3}\left(\frac{\epsilon_0}{j_i}\right)^{1/2}\left(\frac{2e}{M}\right)^{1/4} V^{3/4} \quad , \tag{14}$$

where j_i is the ion current density, V is the potential drop across the sheath, and M is the ion mass.

Variation of the sheath potential will cause the sheath edge to move backwards and forwards with a velocity, v_s, given by

$$v_s = \left[\frac{1}{2}\left(\frac{\epsilon_0}{j_i}\right)^{1/2}\left(\frac{2e}{M}\right)^{1/4} V_0^{-1/4}\right]\frac{dV}{dt} \quad . \tag{15}$$

This gives rise to a conduction current in the plasma, and by continuity a displacement current, $i_D (\equiv A\, n_0 e\, v_s)$, in the sheath. By Eq. (11), then, we have

$$C_e(V_0) = \frac{An_0e}{2}\left(\frac{\epsilon_0}{j_i}\right)^{1/2}\left(\frac{2e}{M}\right)^{1/4} V_0^{-1/4} \quad , \tag{16}$$

where A is the surface area of the probe.

It will be remarked that there is some inconsistency in our assumptions near the sheath edge. Equation (14) will break down since n_0 is not infinite there. At the sheath/plasma edge a more reasonable approximation is to assume that all ions arrive with energy (eV_i) . This allows us to define floating potential, V_f , by

$$\left(\frac{2V_i}{M}\right)^{1/2} = \left(\frac{V_e}{2\pi m}\right)^{1/2} \exp\left(-\frac{V_f}{V_e}\right) \quad . \tag{17}$$

We may assume as a suitable criterion for the probe sheath formation the Bohm expression[11] $V_i \approx 0.5\, V_e$. For mercury-vapor this gives $V_f = 5.5\, V_e$. Substituting this for V_0 in Eq. (16), and introducing the electronic Debye length, λ_D , leads to

$$C_e(V_f) = \left[\frac{m}{2M} \exp\left(\frac{V_f}{V_e}\right)\right]^{1/2} \left[\frac{\pi}{\left(\frac{V_f}{V_e}\right)}\right]^{1/4} \frac{\epsilon_0 A}{\lambda_D} = 0.39\left(\frac{\epsilon_0 A}{\lambda_D}\right) \quad , \tag{18}$$

where the numerical value is appropriate to mercury-vapor, and implies that at floating potential the sheath behaves like a parallel-plate capacitor with separation $2.6\, \lambda_D$.

As the basis of Model II, we note that[3]

$$\frac{dD}{dV} \equiv \frac{dD}{dr}\,\frac{dr}{dV} \equiv \frac{\rho}{(dV/dr)} \quad , \tag{19}$$

where ρ is the charge density in the plasma. Evaluated at the probe surface $(r = 0)$, this becomes

$$\frac{C_e(V_0)}{A} = \left[\frac{\rho}{dV/dr}\right]_{r=0} . \qquad (20)$$

Next we must determine ρ and dV/dr. The ion density, n_i, in the sheath will be given in terms of that at the edge, n_0, by

$$n_i = n_0 \left(\frac{V_i}{V_i - V}\right)^{1/2} . \qquad (21)$$

The electron density, n_e, is not given strictly by Boltzmann's law unless the probe is a perfect reflector. So that ρ can be evaluated correctly at the probe surface, we note that the electron density in plane geometry is given by

$$n_e = \frac{n_0}{2} \exp\left(\frac{V}{V_e}\right) \left[1 + \frac{2}{\pi^{1/2}} \int_0^{y_0} \exp(-y^2)\, dy\right] , \qquad (22)$$

where y_0 has been written for $[(V + V_0)/V_e]^{1/2}$ and V is, of course, negative in the electron repelling region.

In determining the electric field at the cathode, which depends on the integral of the charge throughout the sheath, it will be a good approximation, however, to employ Boltzmann's law if $|V_p| \gtrsim (2V_e)$. The error in local electronic charge will be only 2 percent at the sheath edge, and 8 percent where $|V| \approx V_e$. We have, then, for Poisson's equation

$$\frac{d^2V}{dr^2} \approx \frac{n_0 e}{\epsilon_0} \left[\left(\frac{V_i}{V_i - V} \right)^{1/2} - \exp\left(\frac{V}{V_e} \right) \right] , \qquad (23)$$

which integrates to

$$\left(\frac{dV}{dr} \right)^2 = - \frac{2n_0 e}{\epsilon_0} \left[2V_i - 2[V_i(V_i - V)]^{1/2} + V_e \left(1 - \exp \frac{V}{V_e} \right) \right] , \qquad (24)$$

where the constant of integration has been obtained by putting $(dV/dr) = 0 = V$ at the sheath/plasma edge.

At the cathode surface, then, we have

$$\left(\frac{dV}{dr} \right)_{r=0} \approx \frac{2V_e}{\lambda_D} \left[\left(\frac{V_i}{V_e} \right) \left(\frac{V_0 + V_i}{V_i} \right)^{1/2} - \left(\frac{V_i}{V_e} + \frac{1}{2} \right) \right]^{1/2} , \qquad (25)$$

where we have introduced the electronic Debye length λ_D . The capacitance is finally

$$C_e(V_0) = \alpha\left(\frac{\epsilon_0 A}{\lambda_D}\right) \quad , \quad \alpha = \frac{\left(\frac{V_i}{V_0 + V_i}\right)^{1/2} - \frac{1}{2}\exp\left(-\frac{V_0}{V_e}\right)}{2\left[\left(\frac{V_i}{V_e}\right)\left(\frac{V_0 + V_1}{V_i}\right)^{1/2} - \left(\frac{V_i}{V_e} + \frac{1}{2}\right)\right]^{1/2}} \quad . \tag{26}$$

For mercury-vapor α is 0.17 at floating potential, which should be compared with the result of 0.39 given by Model I. It will be noted from Eq. (26) that α is very insensitive to the exact value chosen for V_i .

III. EXPERIMENTS

The experiments were carried out in the mercury-vapor discharge tube of Fig. 1 at a pressure of about 10^{-3} mm Hg. Seven probes of different shapes and sizes were available, as detailed in Table I. The supports of the cylindrical probes were screened (see Fig. 2). The probe/screen capacitance, C_{AB} , was eliminated from the impedance measurements by including it in the bridge balance with the plasma off. Probe 4 was covered with a thin insulating layer of alumina to avoid perturbing the longitudinal potential gradient in the tube.

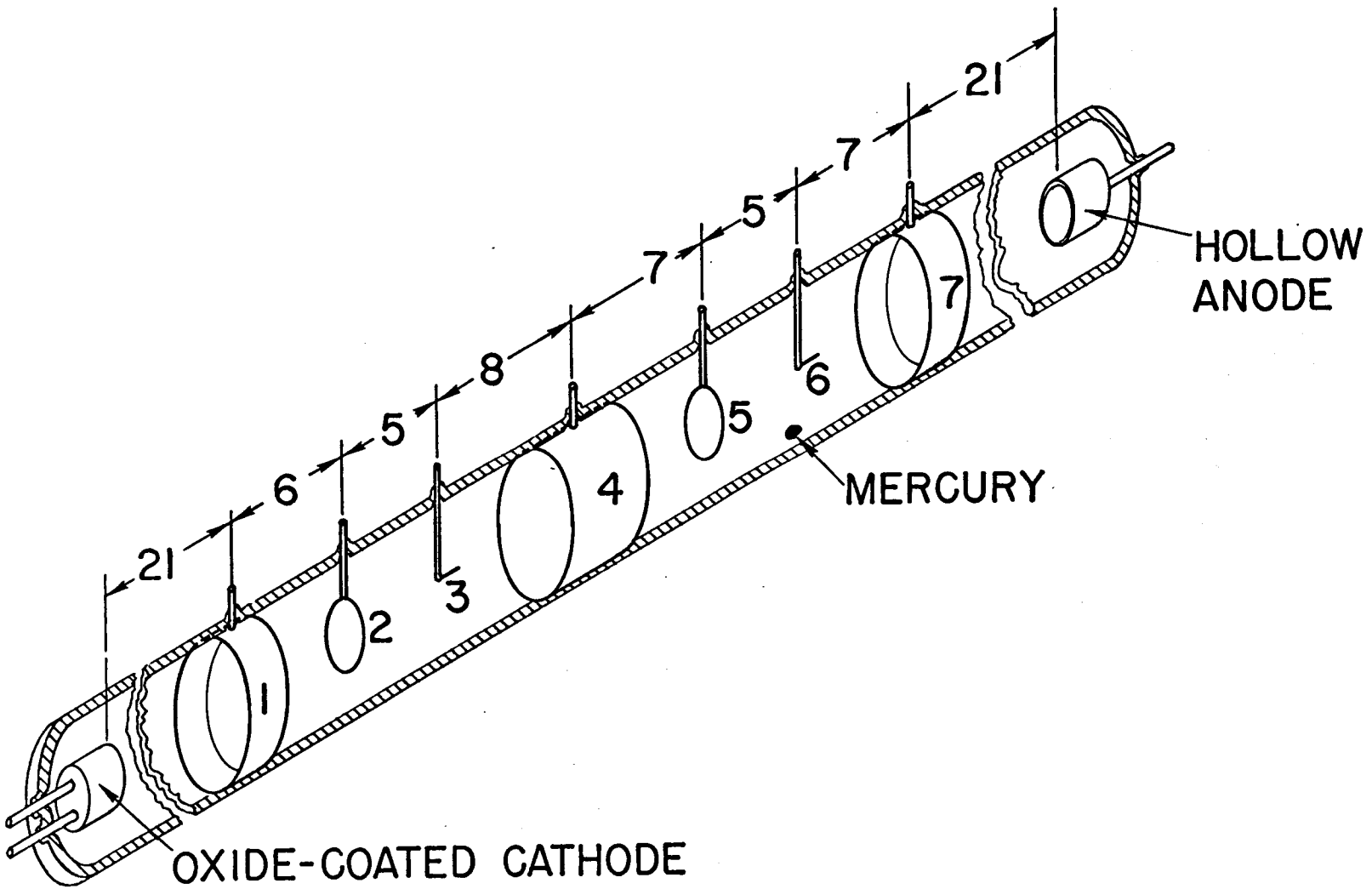

FIG. 1--Experimental mercury-vapor discharge tube. (Dimensions in cm. Tube inside diameter 6 cm.)

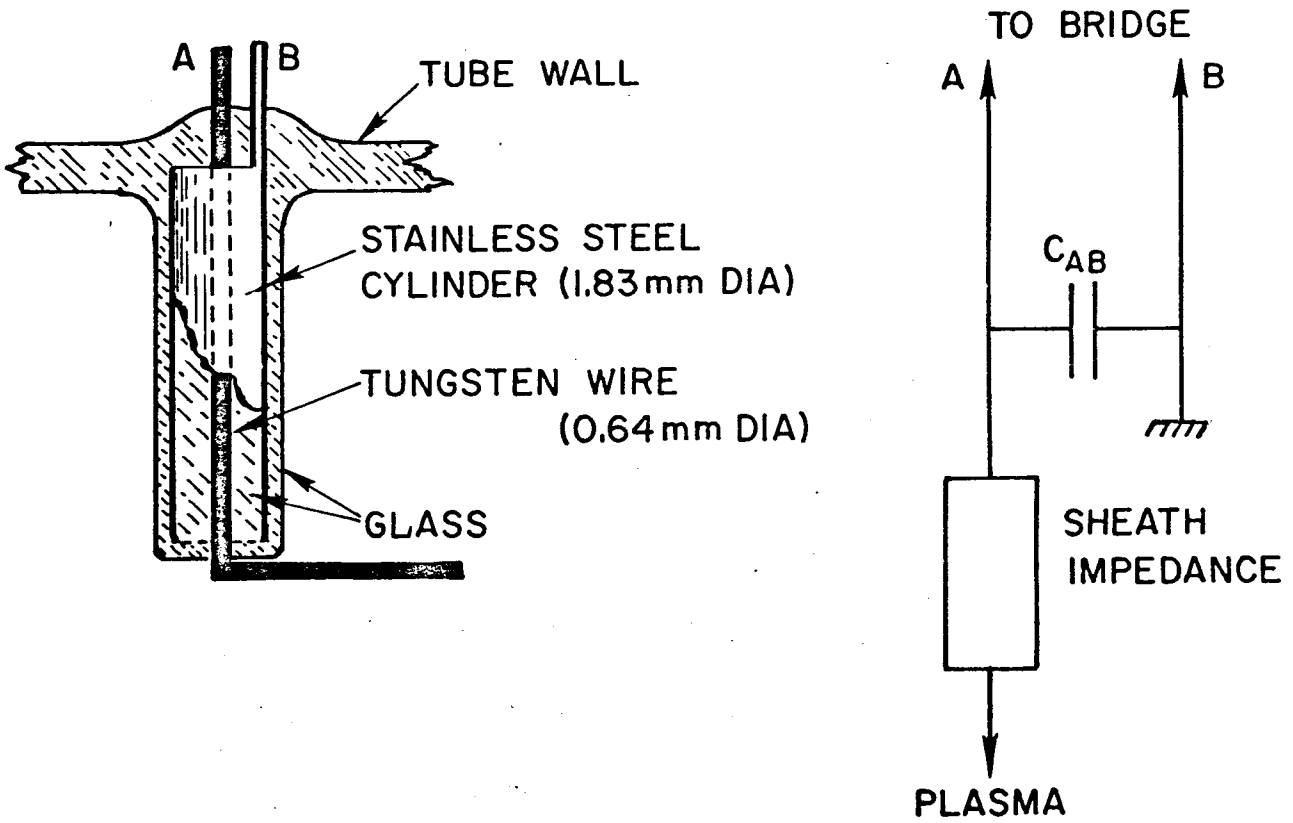

FIG. 2--Screened probe and equivalent circuit.

TABLE I

Details of the Probe Electrodes

Probe geometry	Planar		Cylindrical			
			Loop		Straight	
Probe number	1,7	4	2	5	3	6
Probe width, or wire diameter, d mm	20	40	2.54	0.254	2.54	0.254
Length, cm	6π	6π	3π	3π	0.75	0.75
Surface area, cm^2	37.7	75.4	7.52	0.752	0.60	0.060
(d/λ_D) at 100 mA tube current	~70	~140	~10	~1	~10	~1

Impedance could be measured over the range 20 kc/s - 5 Mc/s by means of a commercial low-frequency bridge. The external connections and equivalent circuits are shown in Fig. 3. The impedance measured between the probe and either the cathode or the anode as reference consists essentially of the probe sheath impedance in series with the plasma impedance, and that of the sheath on the reference electrode. The latter is negligible for probes 3, 5 and 6 at all potentials and for all probes at floating potential. The plasma itself can be assumed to a good approximation to be a perfect conductor.

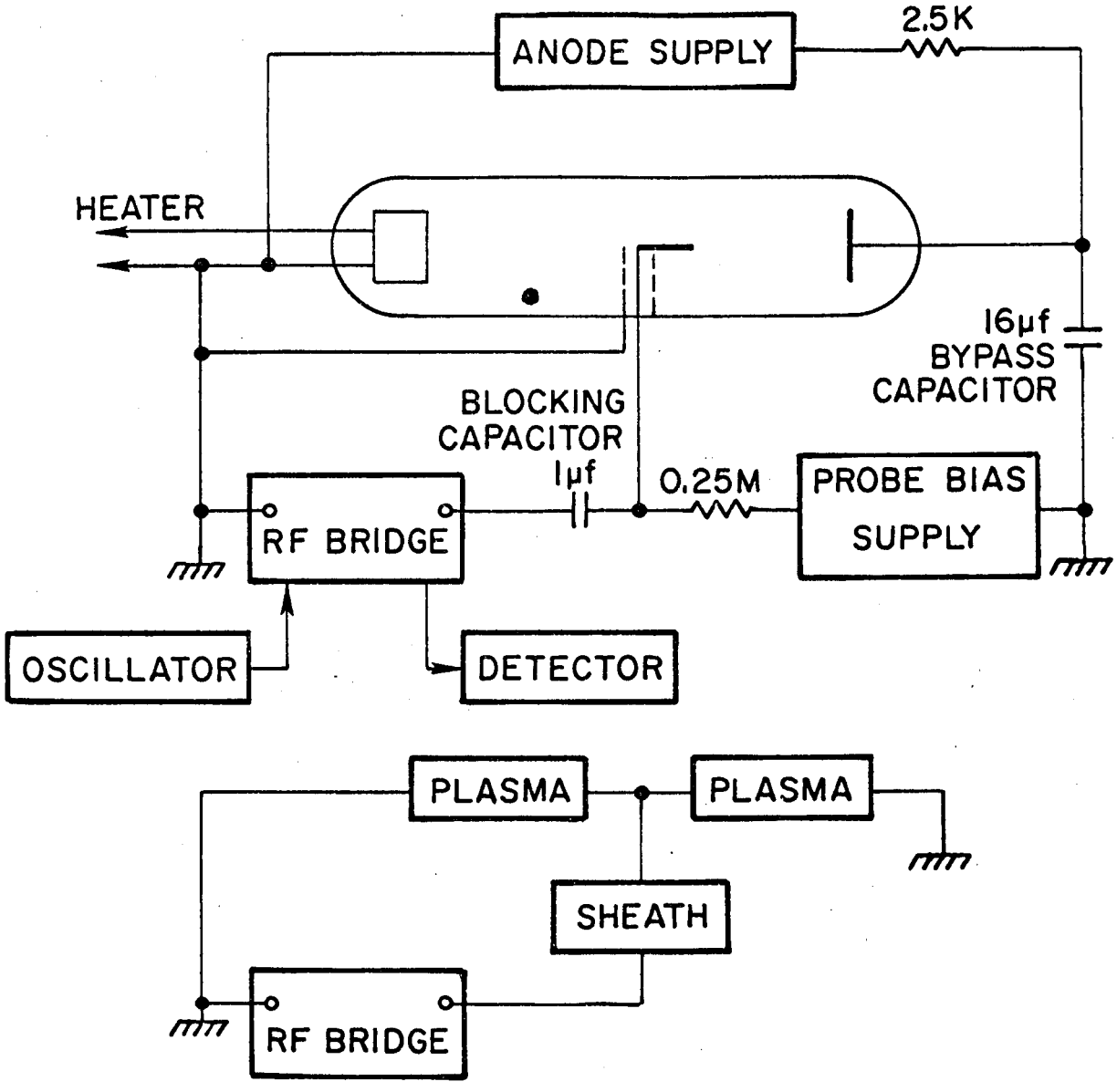

FIG. 3--Impedance measuring circuit and equivalent circuit elements.

Preliminary experiments using the conventional Langmuir technique indicated consistency among determinations of the plasma parameters for probes 3, 5 and 6. Electron saturation current could not be reached for the others because of their large collecting areas. Typical plasma parameters were $V_e \approx 1.9$ volts, and $n_0 \approx 1.3 \cdot 10^9$ per cm^3 on the tube axis. The corresponding Debye length, 0.28 mm, has been used to compute the last line of Table I. The effect of the earth's magnetic field may be neglected in these experiments since the electron gyroradius (~10 cm) is much larger than the Debye length. Collisions in the sheath may also be neglected since the electron/neutral mean free path is long compared to the sheath dimensions, which will be of the order of a few Debye lengths.

A. CONDUCTANCE MEASUREMENTS

The most important features of Eq. (9) for the conductance are that it predicts (i) frequency-independence, (ii) direct proportionality to tube current, and (iii) inverse proportionality to electron temperature. Experiments were carried out to verify these points:

First, the conductance components of cylindrical and planar probes were measured over a range of frequency extending from the lower limit set by the possibility of obtaining an accurate null of the bridge detector up to frequencies well in excess of the ion plasma frequency. Typical results are shown in Fig. 4, and confirm (i) . Next, experimental checks on the validity of (ii) yielded supporting results such as those shown in Fig. 5. These confirm, incidentally, that the conductance is not geometry-dependent. Finally, comparisons were made

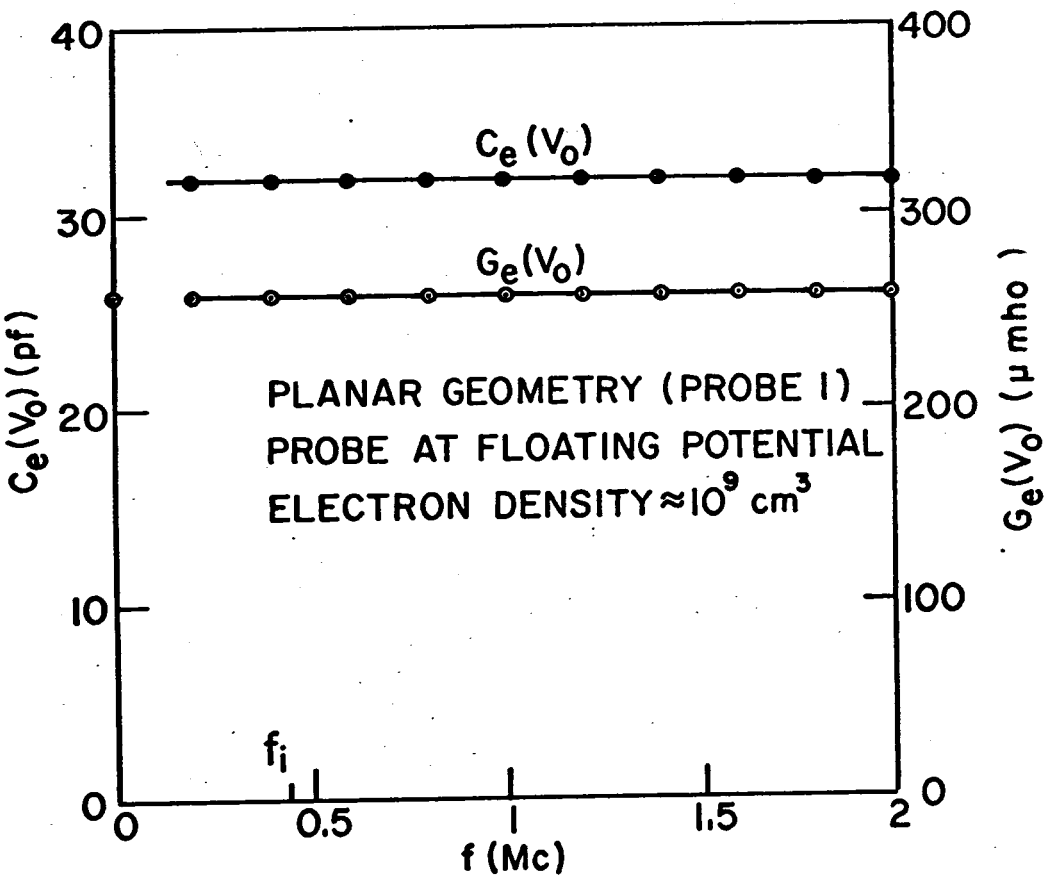

FIG. 4--Variation of probe conductance and sheath capacitance with frequency. (The point "f_i" indicates the ion plasma frequency.)

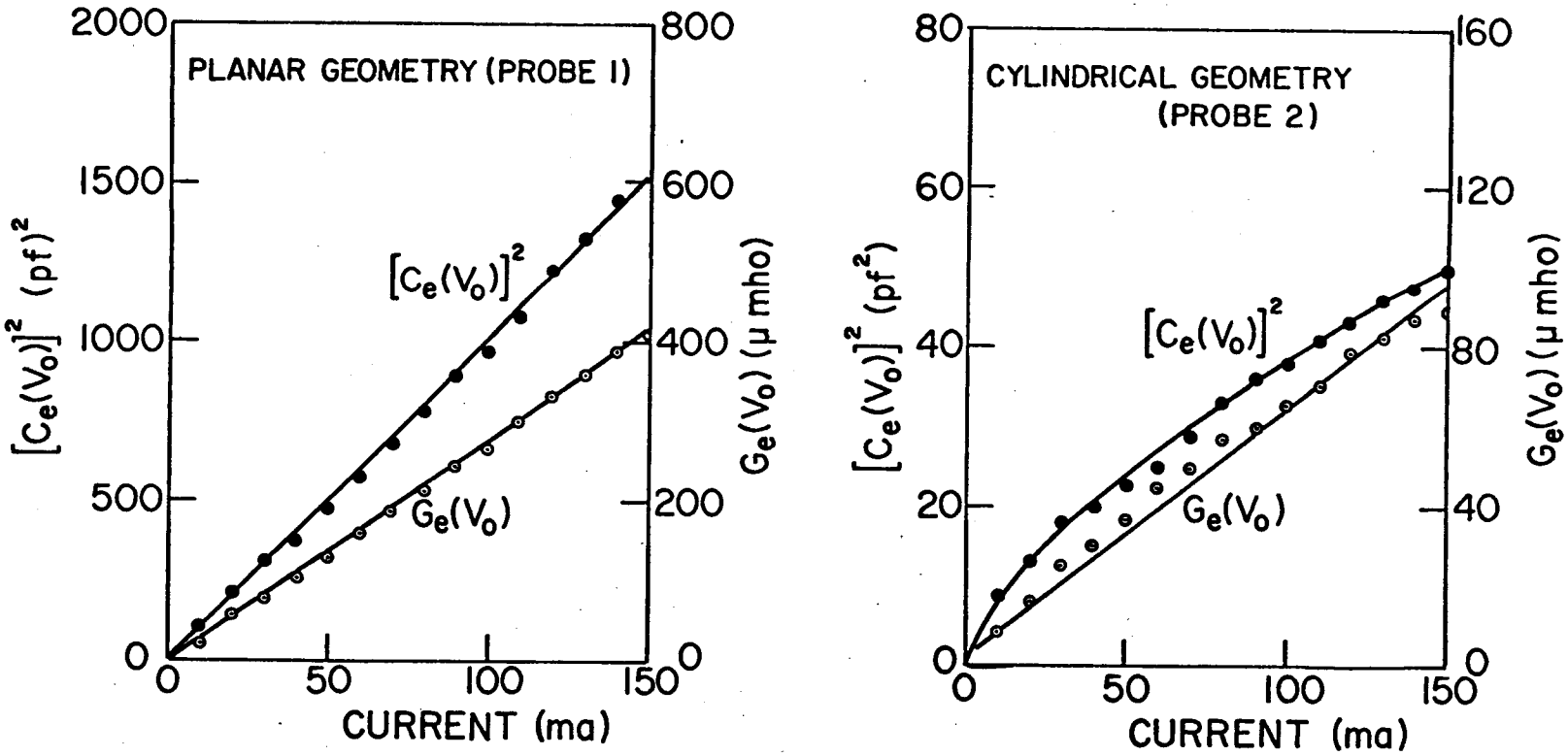

FIG. 5--Variation of probe conductance and capacitance with discharge current. (Working frequency 500 kc/s. Probes at floating potential.)

between conductance characteristics and Langmuir probe characteristics taken under the same conditions. These were confined to the smallest probes because it was necessary to be able to reach saturation. Figure 6 shows typical results. The experiments indicate agreement to within 10 percent between measured values of conductance and those obtained by graphical differentiation of the dc Langmuir probe characteristic. The temperature obtained from the slope of the conductance characteristic and the semi-logarithmic plot agreed to the same limits. As far as determination of space potential is concerned, we may remark that there is generally a marginal advantage in using the conductance variation to locate this point. Ideally, a sharp change of conductance should occur at space potential. In practice there is a knee, but the "break-point" can be located more accurately on a linear conductance plot than on a semi-logarithmic dc probe characteristic. Figure 6 indicates this for a cylindrical probe.

B. CAPACITANCE MEASUREMENTS

Equations (18) and (26) indicate that the capacitance should be: (i) frequency-independent over the ranges of validity of these expressions, and (ii) inversely proportional to Debye length. This latter condition may be expressed as direct proportionality of $[C_e(V_0)]^2$ to the discharge current. Series of experiments were carried out to verify these points. Figure 4 indicates frequency independence from about 0.2 f_i to well above f_i. This implies that rf ion motions are negligible and inclines us towards Eq. (18). Experiments could

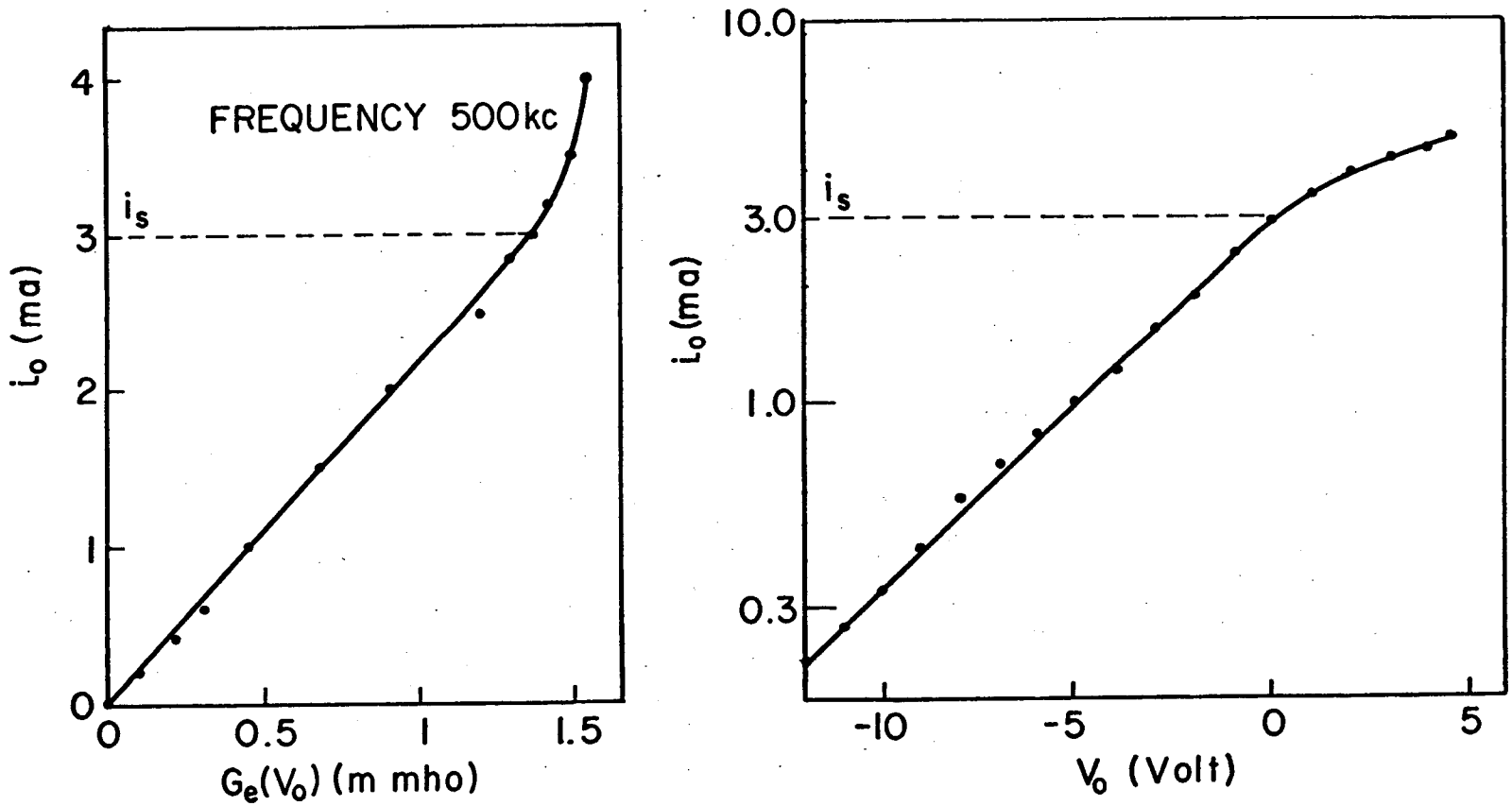

FIG. 6--Comparison of conductance and conventional Langmuir probe characteristics (Cylindrical geometry. Probe 5.)

not be carried out at lower frequencies owing to difficulties in obtaining an accurate null of the bridge due to noise from the discharge. There was also a high ratio between the admittance components which made susceptance measurements difficult. Figure 5 shows the effect of current variation. For the planar probe, which is large compared to a Debye length, we see that (ii) is satisfied. For the cylindrical probe whose diameter does not greatly exceed the sheath thickness, the required proportionality breaks down.

Finally, a direct check on the value of the capacitance is required. Some typical measurements obtained at floating potential are tabulated below. As expected, the predictions of Eqs. (18) and (26) bracket the experimental values for the three probes for which the planar theory is appropriate. The discrepancies from Model I are 30 percent or less, and are rather larger from Model II. These are the combined errors due to simplifications in the theory, and errors in making the conventional Langmuir probe data reduction on which the comparison is based.

TABLE II

Predicted and Measured Values of Probe Capacitance at Floating Potential (i_a = 100 mA)

Probe	1	7	2	5
Debye length λ_D mm	0.365	0.365	0.311	0.311
Measured capacitance $C_e(V_f)$ pF	32	25	6.3	2.4
$C_e(V_f) \Big/ \left(\frac{A\epsilon_0}{\lambda_D}\right)$	0.35	0.27	0.29	1.12

IV. DISCUSSION

The experiments indicate that the conductance measurement technique can give electron density and temperature information to about the same accuracy as the usual semi-logarithmic plot of probe current and potential. Apart from a slight advantage in the determination of space potential, the only situations in which the method might prove more convenient are probably those in which telemetering is involved.

The admittance measurement technique has the advantage that no sweeping of the probe potential is required. It is consequently most suitable for continuous measurement in time-varying laboratory or space

plasmas. Operation at floating potential is particularly convenient, but is only appropriate where the electron velocity distribution is approximately Maxwellian up to energies corresponding to floating potential. If the probe potential is reduced this requirement becomes less stringent, but the theory of the probe capacity becomes more complicated. Since only low electron and ion currents are taken at space potential, very large probes can be used, and the technique may have useful applications to measurements in very low density plasmas.

As far as the applicability of the results in this paper to the impedance measurements already carried out in space is concerned, it seems that an extension of the theory to cover the influence of a magnetic field is required. Further experiments in drifting plasmas should be carried out to simulate conditions pertaining to a moving space vehicle. This is particularly important since transit time phenomena, which have been neglected so far, will appear when distances traveled by the particles during one period of the signal applied to the probe are no longer negligible with respect to the size of the probe. Such conditions will be approached frequently in space applications.

REFERENCES

1. K. Takayama, H. Ikegami and S. Miyasaki, Phys Rev. Letters 5, 238 (1960);
   R. S. Harp and F. W. Crawford, J. Appl. Phys. 35, 3436 (1964);
   F. W. Crawford and R. S. Harp, J. Geophys. Res. 70, 587 (1965);
   F. W. Crawford, Microwave Laboratory Report No. 1279, Stanford University (December 1964).
2. R. F. Mlodnosky and O. K. Garriott, Proc. International Conference on the Ionosphere, London, July 1962 (Bartholomew Press, Dorking, England) p 484.
3. F. W. Crawford and R. F. Mlodnosky, J. Geophys. Res. 69, 2765 (1964).
4. Stanford Research Institute, Menlo Park, California (to be published).
5. P. E. Crouse, Ionosphere Res. Lab., Scientific Report No. 208, Pennsylvania State University (May 1964).
6. F. W. Crawford, J. Appl. Phys. 33, 20 (1962).
7. F. W. Crawford, J. Appl. Phys. 34, 1897 (1963).
8. L. B. Loeb, Basic Processes of Gaseous Electronics (University of California Press, Berkeley, California, 1955) pp. 361-370.
9. L. Tonks and I. Langmuir, Phys. Rev. 34, 876 (1929).
10. H. S. Butler and G. S. Kino, Phys. Fluids 6, 1346 (1963).
11. D. Bohm, The Characteristics of Electrical Discharges in Magnetic Fields, ed. Guthrie and Wakerling (McGraw-Hill Publishing Co., Inc., New York, 1949) Chapter 3.